



Cite this: *Sens. Diagn.*, 2024, **3**, 1263

## Synthesis and fluorescence properties of 2'-benzyloxy flavone—a dual probe for selective detection of picric acid and pH sensing†

Vengatesh Gopal,<sup>a</sup> Jayasankar Sudhakaran, <sup>a</sup> Nirenjana Ramachandran,<sup>a</sup> Thejus Kozhiyottu Mana,<sup>a</sup> Aravind Remesh Kana,<sup>a</sup> Anandhu Omanakuttan Nair,<sup>a</sup> Priyanka Mohan,<sup>a</sup> Tejaswini Madhusudhan,<sup>a</sup> Sankarasekaran Shanmugaraju <sup>\*c</sup> and Pandurangan Nanjan <sup>\*ab</sup>

Flavonoids are naturally occurring oxygen-containing heterocyclic systems with unique properties for diverse applications. The present study reports the synthesis of a new 2'-benzyloxy flavone and explores its fluorescence sensing properties towards secondary chemical explosives, such as picric acid, and pH sensing. The target 2'-benzyloxy flavone fluorophore (5) was synthesized in three-step reactions with good yield and was fully characterized using NMR, FTIR spectroscopy, and HRMS. The sensing propensity of 5 towards nitroaromatics and pH was probed using fluorescence spectroscopy. Compound 5 exhibited a preferential sensing property for phenolic nitroaromatics with high quenching efficiency for picric acid and differential fluorescence responses for different pH. The superior selectivity of 5 for picric acid is attributed to the intermolecular hydrogen bonding interactions between the O atoms in 5 and the OH groups of picric acid. The observed experimental results were further validated by computational calculations which strongly supported the hydrogen-bond-driven sensing selectivity. Furthermore, selective sensing of picric acid by 5 was further demonstrated in real-water samples and using paper-based sensing. These studies make compound 5 a potential dual sensor for selective sensing of picric acid and sensing of pH of the medium.

Received 9th May 2024,  
Accepted 20th June 2024

DOI: 10.1039/d4sd00151f

rsc.li/sensors

## 1. Introduction

The strategic design of selective small-molecule sensors is always challenging and assumes a special interest in material and biomedical fields.<sup>1–4</sup> In particular, neutrality-based small-molecule sensors for nitroaromatics (NAs) have attracted interest recently and form an active area of research.<sup>5–7</sup> One such fluorescence property has been found in flavonoids. Flavonoids are polyphenolic secondary metabolites and are known for their unique structural organization and properties, such as amphiphilicity, multi-functionality, biocompatibility, and dual resonating behavior.<sup>8,9</sup> In flavonoids, flavones (2-phenyl-1-benzopyran-4-one) form a subclass that contributes significantly to the flavonoid family. The flavone structure shows two characteristic absorption

peaks due to the conjugation of the A-ring (250–270 nm, band I) and B-ring (310–350 nm, band II) with the carbonyl group (Scheme 1).<sup>10</sup> To our knowledge, flavones are not identified as sensors for nitroaromatics. However, only one example is reported for flavonol to sense picric acid. The sensing behavior of flavonol is due to its excited state intramolecular proton transfer (ESIPT) process.<sup>11</sup>

Flavonol possesses weak fluorescence due to hydroxyl (acts as a donor) and carbonyl (acts as an acceptor) in the  $\alpha$  and  $\beta$  positions. Additionally, another activating linker or fluorescently active group must be introduced to make flavonol an effective fluorophore (only flavonol was reported for picric acid quenching).<sup>12</sup> On the other hand, flavones have been attractive for their uniqueness, *i.e.* they are abundant, easy to synthesize, functionally tunable, non-toxic, and biologically active.<sup>13</sup> In the present study, it has been identified that 2'-

<sup>a</sup>Department of Sciences, Amrita School of Physical Sciences, Amrita Vishwa Vidyapeetham, Mysore, India. E-mail: [n\\_pandurangan@cb.amrita.edu](mailto:n_pandurangan@cb.amrita.edu)

<sup>b</sup>Department of Chemistry, Amrita School of Physical Sciences, Amrita Vishwa Vidyapeetham, Coimbatore, India

<sup>c</sup>Department of Chemistry, Indian Institute of Technology Palakkad, Palakkad, 678557, Kerala, India. E-mail: [shannugam@iitpkd.ac.in](mailto:shannugam@iitpkd.ac.in)

† Electronic supplementary information (ESI) available. See DOI: <https://doi.org/10.1039/d4sd00151f>



**Scheme 1** Resonance and electron-transfer process of flavones.



benzyloxy flavone is a neutral quencher for nitroaromatics. Another study by Yang's group reported nitroaromatic sensing in a neutral system.<sup>2</sup> Thus, the identification of selective sensing of nitroaromatics (NAs) is important because they can cause eye irritation, skin allergy, dizziness and nausea and can damage the liver and kidney. It is further identified that over-exploitation of nitroaromatics threatens humans by affecting the environment.<sup>14–17</sup> Hence, developing a new fluorophore for trace or *in situ* detection of nitroaromatics (explosives, pesticides, and antibiotics) is an attractive and vital area of research in environmental and national security applications. There is a plethora of materials, such as different polymers, porous organic materials (COFs and MOFs), luminescent gels, macromolecules, quantum dots, and dendrimers, that have been discovered for the trace detection of nitroaromatics.<sup>18</sup> However, their preparation is challenging. Recently, small-molecule fluorophores (with neutral behavior) have attracted much attention for the detection of NAs.<sup>19</sup> In most cases, the NA sensors are designed based on attaching fluorophore linkers with electronically rich polyaromatics or tertiary amine-based molecules.<sup>18</sup> Based on the uniqueness of flavone and the necessity for detecting NAs, we synthesized a novel fluorophore for detecting NAs, in particular picric acid.

Further, the development of pH sensors is essential and often required for analyzing different materials from food, chemical, medical, biological, environmental sources, etc.<sup>20–23</sup> The pH sensors are broadly classified into two, *i.e.*, electrochemical and fiber optic sensors.<sup>24–26</sup> Although these two sensors have several applications, they lack vast generality due to various interferences.<sup>27</sup> Among these techniques, fluorescent pH sensing has attracted considerable attention due to its high sensitivity and faster reaction time.<sup>28</sup> For example, the study by Sun's group reported that the novel pyrene-based fluorescence pH sensor is in the biological system.<sup>7</sup> Therefore, finding novel fluorophores with good sensitivity and photostability in more extended pH ranges is always essential and considered as an important area of research. Based on these structural insights, we developed fluorophores for pH sensing. The synthesized compound has also been used for the sensing of different pHs, from acidic (pH 1–6) to alkaline (pH 8–14) conditions. To the best of our knowledge, this is the first example of an oxygen-containing heterocycle (without fluorophore moiety): 2'-benzyloxy flavone, an electronically rich dual fluorophore for trace detection of nitroaromatics (picric acid) and pH sensing. In addition, portable, cost-effective, and “point-of-care” devices for any diagnostics have become important in recent years due to their industrial/commercial applications.<sup>29–31</sup> With that in view, the study has also explored paper-based fluorescence systems for this dual behavior.

## 2. Experimental

### 2.1. General information

All reagents utilized for synthesis and analysis were purchased from various industries, such as Sigma Aldrich,

Spectrochem, and Avra. All the analytical experiments were carried out using HPLC-grade MeOH. Absorption measurements were carried out using a Lab India 3100-XE UV/vis spectrophotometer. A Shimadzu FR-6000 Spectro fluorophotometer was used for fluorescence measurements and maintained a 5 nm slit width for both emission and excitation. <sup>1</sup>H synthesised compounds were characterized by NMR (Bruker; 400 MHz instrument and TMS used as internal standard) and mass spectroscopy (Agilent 1100 Series; ESI-MS with positive ion mode on a liquid chromatography-ion trap mass spectrometer).

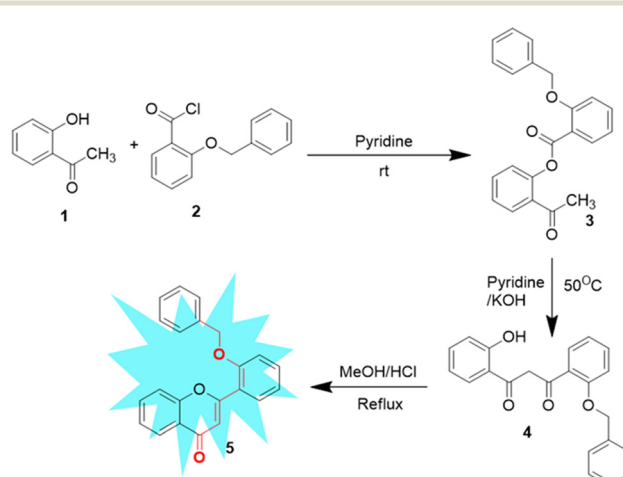
### 2.2. Synthetic protocol

Synthesis of 2'-benzyloxy flavone was performed according to a procedure reported previously by our group *via* a modified Baker–Venkataraman reaction.<sup>32</sup> The base-catalyzed response of 2'-benzyloxy acetophenone (3) to 1,3-diketone (4), followed by acid-catalyzed cyclodehydration, gave flavone fluorophore (5) in a good yield. All the synthesized compounds were subjected to spectroscopic identification, which is given below (Scheme 2).

**2-Acetylphenyl-2-(benzyloxy)benzoate (3).** Yield 85%: <sup>1</sup>H NMR ( $\text{CDCl}_3$ )  $\delta$ : 2.46, s, 3H; 5.14, s, 2H; 6.99, m, 2H; 7.11, dd, 1H; 7.20, m, 2H; 7.28, m, 3H; 7.41, m, 2H; 7.7, dd, 1H; 8.04, dd, 1H. <sup>13</sup>C NMR ( $\text{CDCl}_3$ )  $\delta$ : 197, 164, 158, 149, 136, 134, 133, 132, 131, 130, 128, 127.8, 127, 126, 124, 120, 119, 113, 70, 29. Mass data [M – H]<sup>–</sup>: 345.12 (exact mass 346.12).

**1-(2-(BenzylOxy)phenyl)-3-(2-hydroxyphenyl)propane-1,3-dione (4).** Yield 78%: <sup>1</sup>H NMR ( $\text{CDCl}_3$ )  $\delta$ : 5.09, s, 2H; 6.46, t, 1H; 6.83, d, 2H ( $J$  = 8.4 Hz); 7.02, dd, 2H; 7.38, m, 2H; 7.41, m, 3H; 8.05, dd, 1H; 12.09, s, 1H; 15.5, s, 1H. <sup>13</sup>C NMR ( $\text{CDCl}_3$ )  $\delta$ : 196, 174, 162, 158, 135.7, 135.2, 133, 130, 128.9, 128.7, 128.6, 121.1, 118.9, 118.3, 112, 97, 71. Mass data [M – H]<sup>–</sup>: 345.32 (exact mass 346.12).

**2.2.1. 2'-BenzylOxy flavone (5).** Yield 72%: <sup>1</sup>H NMR ( $\text{CDCl}_3$ )  $\delta$ : 5.18, s, 2H; 6.99, m, 2H; 7.16, d, 2H ( $J$  = 6.4 Hz); 7.24, d, 1H ( $J$  = 6.8 Hz); 7.3, t, 1H; 7.33, m, 4H; 7.43, d, 1H ( $J$  = 8.4



**Scheme 2** Synthesis of the fluorophore, 2'-benzyloxy flavone.



Hz); 7.61, t, 1H; 7.77, dd, 1H; 8.16, dd, 1H.  $^{13}\text{C}$  NMR ( $\text{CDCl}_3$ )  $\delta$ : 178, 162, 157, 156, 136, 133, 132, 129, 128.7, 128.1, 127, 125.7, 125.1, 123, 121.4, 121.1, 118, 113, 112, 70. Mass data  $[\text{M} + \text{H}]^+$ ; 329.35 (exact mass 328.11).

### 2.3. General procedure for sensing studies

UV-vis absorption measurements were recorded on a spectrophotometer. A methanolic solution of samples was used for the fluorescence analysis. The fluorophore was taken in a millimolar concentration. The flavone solution was titrated against PA (4 nM to 299 nM) with increasing concentrations. A significant spectral change was observed with and without picric acid. All the spectra were exploited to obtain the complete profile. Whatman paper was immersed in the flavone solution (0.01 mM) for 30 s and then dried in air. The test papers were then immersed in a picric acid-containing aqueous solution for 2 min and then air-dried to detect picric acid in actual samples. Similarly, the experiments were repeated for pH sensing. Tap, drainage, and distilled water were used to prepare actual samples. Firstly, the collected water was filtered with Whatman filter paper to remove solid contaminants. Then, it was spiked with PA and taken for fluorescence analysis.

### 2.4. Computational calculations

The frontier molecular orbital (FMO) is essential for UV-vis spectra, chemical reactions, and the investigation of the optical and electronic properties of molecules.<sup>33–37</sup> The fluorescence quenching mechanism of flavone was studied by adding picric acid (PA), proton, and hydroxy groups identified using the Gaussian 09 program. Structure optimization was done using the DFT-B3LYP, 6-311G(dp) basis set. TD-DFT calculations on the optimized geometries of flavone using the above basis sets were carried out to obtain information about absorption and emission. The obtained results were plotted using GaussView 05 with the isosurface value 0.02.

## 3. Results and discussion

Flavone chemistry inspired us to explore fluorophore development for various sensing applications. After understanding the resonating behavior of the flavone, the B-ring was identified for modification and its effect on fluorescence-based sensing was investigated. For that, we chose the 2'-position of flavone for its electron-donor nature and carbonyl as an electron acceptor, which leads the UV absorption band at the 300–350 nm region.

### 3.1. Fluorescence sensing of picric acid by 2'-benzyloxy flavone

After the successful design and synthesis of the fluorophore, it was subjected to solvatochromic study using a non-polar to polar solvent medium (Fig. 1b). Further, it was identified that the flavone fluorophore showed maximum ( $\lambda_{\text{max}}$ ) fluorescence

absorption at 310 nm and emission at 427 nm (Fig. 1a). The analysis found that methanol gives the best absorption compared to other solvents listed in Fig. 1b and no absorption was found in toluene. The interaction of 2'-benzyloxy flavone with picric acid (PA) was analyzed in MeOH solvent. The absorption spectrum showed a distinct shift from 310 nm to 330 nm when PA was added (as indicated in Fig. 2). The fluorescence spectrum showed an excellent response to PA in nanomolar concentrations. From fluorometric titration, it was observed that the fluorescence intensity decreased with increasing concentrations of PA. Thus, the fluorescence quenching process (at 430 nm) was observed between the fluorophore and the analyte (Fig. 2). The resulting solution was found to be stable even after a month, suggesting a strong interaction with PA, which is very unlikely compared to standard sensing mechanisms. Moreover, a colorless to pale yellow color change was noticed due to the formation of the proton transfer complex between PA and the flavone sensor. Interestingly, the calculated quenching efficiency (95%) of the flavone sensor is on par with that of other reported sensors,<sup>11,12</sup> indicating the efficiency of flavone detection of PA even at low concentrations. From the analysis, PA's detection limit (LOD) was estimated as 4 nM. Further, the Stern–Volmer plot suggested that the quenching mechanism was static which is further supported by literature reports.<sup>38,39</sup>

### 3.2. pH sensing properties of 2'-benzyloxy flavone

The experimental study started under acidic pH conditions (see Fig. 3). Analysis showed that until pH 5 there were few changes (only a 1-fold increase) in the intensity. When the pH reached 4, there was a considerable increase (6-fold increase) in the absorption. Further, the maximum increase (10-fold increase) in the intensity was found at pH 3, followed by a decrease in the intensity to its original absorption. From the analysis, it could be deduced that the designed sensor could be helpful in the pH 3 to pH 4 regions (Fig. 3). Similarly, the sensor was also studied at basic pH 7–14. Unlike acid sensing, base sensing showed a systematic increment in the fluorescence intensity. However, it gave the best response at pH 14 with an increase in the intensity by 23-fold. Both analyses identified that the designed sensors could be utilized to study wide ranges of pH (Fig. 3).

### 3.3. Fluorophore quenching of picric acid in various water solutions

The study was further extended to identify picric acid in various water media collected from different sources. The study indicated no substantial differences in the quenching of picric acid in sewage and tap water. However, there is a slight variation in the pure water (distilled water) sample (indicated in Fig. 4), which suggests that variation in pH may affect the quenching as in the case of distilled water, pH may be slightly acidic, confirming that the fluorophore gives



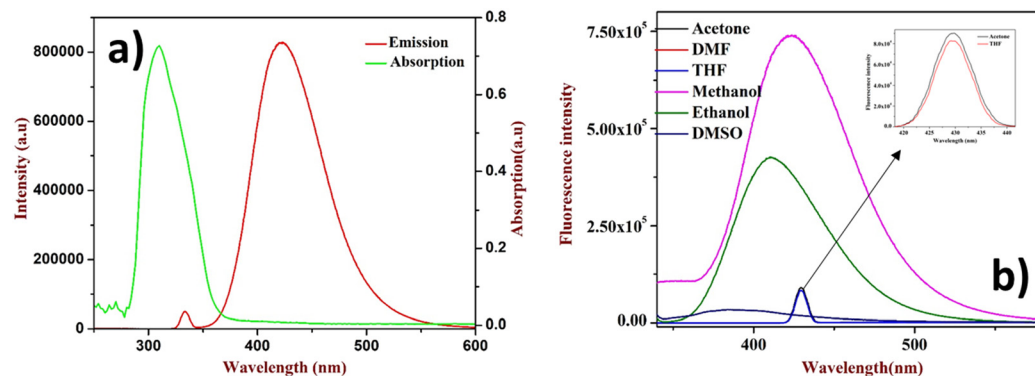


Fig. 1 (a) UV absorption and emission of 2'-benzyloxy flavone, (b) solvatochromism study (inset: THF and acetone only show less absorption).

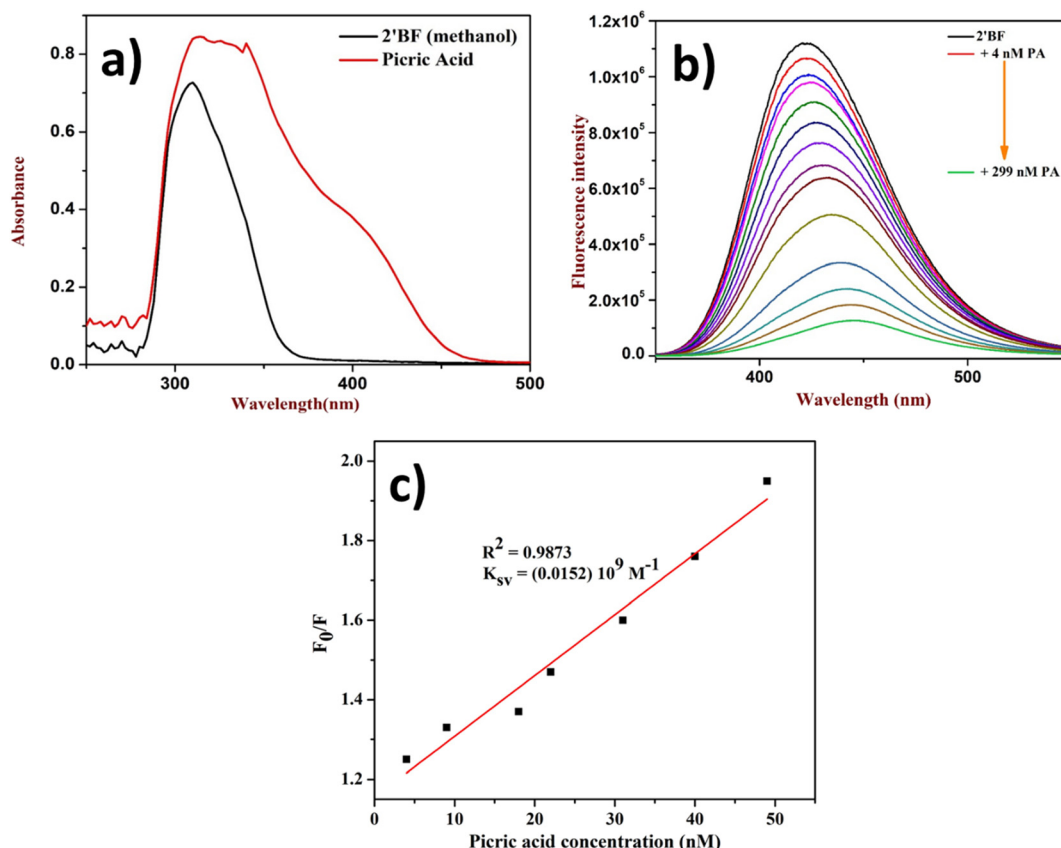


Fig. 2 Quenching study of 2'-benzyloxy flavone with PA: (a) fluorophore with PA in UV, (b) titration of PA, and (c) Stern–Volmer plot.

enhancement with lower pH. The analysis suggested no interference was observed even in the real sample analysis.

This unique feature is essential and can be considered for effective probe development for environmental applications.

### 3.4. Analysis of dual sensing properties on test strips

An effort was also made to prepare paper-based test strips for picric acid and pH sensing studies. For this, Whatman paper was dip-coated in a solution of 2'-benzyloxy flavone, then

dried under atmospheric conditions (control sample). The sensors at pH 3 and pH 5 were taken in a separate paper and dried similarly (fluorescence enhancement). In the same way, the PA (with varied concentrations) quenching solution was also taken in another paper and dried accordingly. Three strips were compared under UV light; a fluorescence enhancement with pH 3 was identified, and quenching with PA was observed (Fig. 5). From the analysis, it is indicated that fluorescence enhancement was observed under different pH conditions and dose-dependent quenching was observed with the various picric acid solutions.

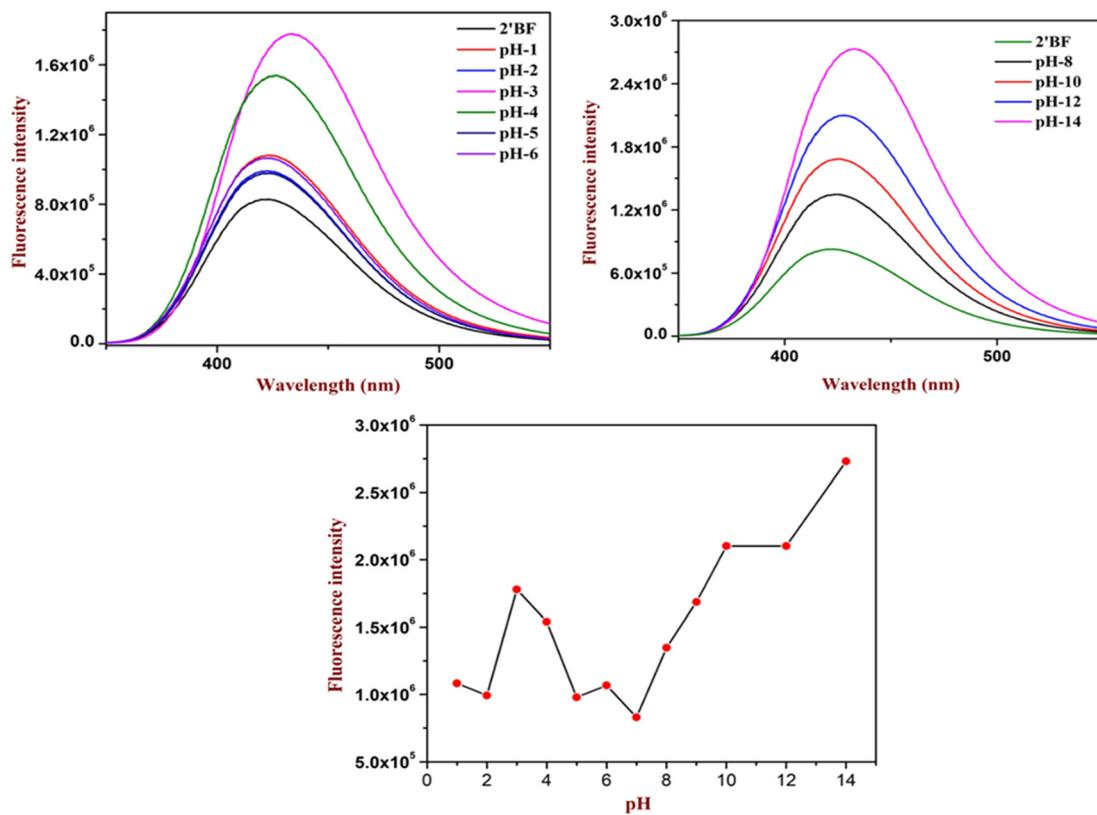


Fig. 3 Quenching study of 2'-benzyloxy flavone with different pH.

### 3.5. DFT calculation of flavone with picric acid

The rationale behind benzyloxy at the 2'-position is that it acts as an electron donor, and the benzene ring improves the  $\pi$ - $\pi$  interaction with the nitroaromatics. Also, it can be easily synthesized. With this perception, DFT calculation was performed with the geometries of flavone and PA adducts, which were initially optimized using known set parameters.<sup>40,41</sup> The charges were calculated on the O atom (carbonyl in the C-ring) of flavone and PA adducts. The DFT-optimized geometry of 2'-benzyloxy flavone and flavone with picric acid is shown in Fig. 6.

The analysis showed that a significant electron density reduction was observed on the O atom of flavone upon

binding of PA, indicating the charge transfer process between flavone and PA (Fig. 6). From the FMO analysis, it is identified that a PA to flavone internal charge transfer (ICT) process has taken place (Fig. 6). In the interaction of 2'-benzyloxy flavone with picric acid, HOMO occupies only picric acid, whereas LUMO electron density spreads over the flavone moiety. Results suggested that after addition of PA, the electron density was significantly decreased in flavone. The result shows that 2'-benzyloxy flavone and picric acid formed an effective charge-transfer complex (Fig. 7). It is also observed that the electron-deficient nitro group can accept the acidic proton ( $\alpha$ -position) near the carbonyl group, which is acting as a proton donor and carbonyl oxygen binds with

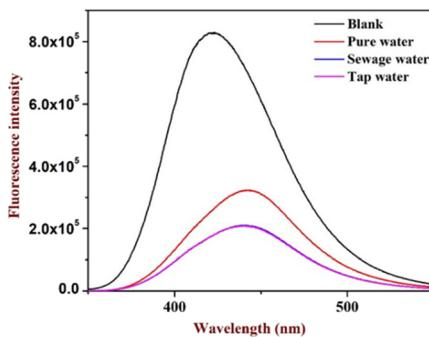


Fig. 4 Quenching studies of picric acid in water.

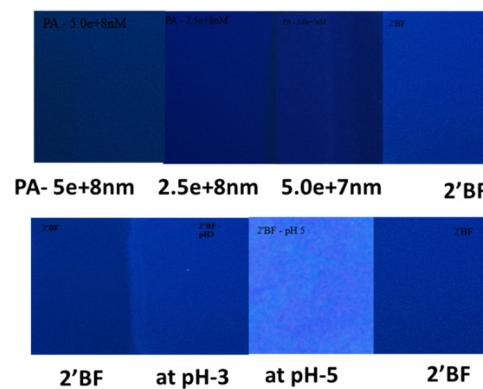


Fig. 5 Dual behavior study on paper strips.

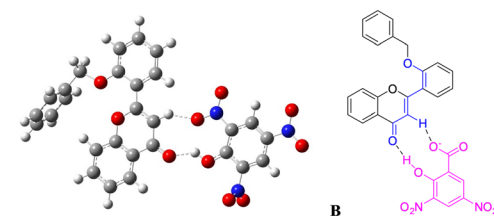


Fig. 6 Interaction of fluorophore with picric acid. (A) Optimized geometry of fluorophore and picric acid and (B) the same interaction representation as a ChemDraw structure.

the acidic proton from picric acid. Further, these interactions stop the electron flow for fluorescence, and the activity is quenched by irreversible picric acid.

The DFT-optimized geometry of 2'-benzyloxy flavone and flavone with picric acid is shown in Fig. 6. The analysis showed that a significant electron density reduction was observed on the O atom of flavone upon binding of PA, indicating the charge transfer process between flavone and PA (Fig. 6). From the FMO analysis, it is identified that a PA to flavone internal charge transfer (ICT) process has taken place (Fig. 6). In the interaction of 2'-benzyloxy flavone with picric acid, HOMO occupies only picric acid, whereas LUMO electron density spreads over the flavone moiety. Results suggested that after adding PA, the electron density was significantly decreased.

### 3.6. DFT calculation of flavone in the presence of acid

Since the flavone carbonyl oxygen is a suitable proton acceptor, the DFT study continued to investigate how acidic protons affect the fluorescence system. The flavone moiety has three acid-accepting sites, which are (i) oxygen in the heterocycle (C ring, Scheme 1), (ii) oxygen present as a carbonyl functionality (C4), and (iii) oxygen (O27) in the benzyloxy system. The heterocyclic moiety's oxygen is omitted due to non-interference in the electron-transfer process. The

carbonyl oxygen and benzyloxy oxygen taken for DFT calculation are indicated in Fig. 8. In the present DFT study, protons were added near the two oxygen atoms separately and the calculations were performed. The analysis revealed that carbonyl oxygen would be ideal for the proton-accepting center, as shown in Fig. 8b. After DFT analysis, the fluorophore was studied under different pHs, starting from pH 6 to 1 (indicated in Fig. 3). The study indicated that, a fluorescence enhancement starts from pH 6. Then, it reached maximum fluorescence absorbance at pH 3. Further, there is a slight decrease in the intensity at pH 2 and pH 1. These results suggested a substantial electron deficiency in carbonyl oxygen when adding a proton. Hence, significant differences were observed at acidic pH with the synthesized fluorophores.

### 3.7. DFT calculation of flavone in the presence of base

The primary system also extends the DFT study by introducing a hydroxyl group on the flavone molecule. It is worth carrying out hydroxyl (OH)-based DFT calculation on flavone since this molecule has different Michael-accepting positions. The alkaline pH study was carried out to understand whether fluorescence quenching is possible by adding OH since it disrupts the electron flow from benzyl to carbonyl. Milliken charge analysis identified that C1, C3, C17, C18, C20, and C31 are more suitable for nucleophilic addition reactions (Fig. 9). These might have acquired electron density due to ring delocalization, except for the C1 carbon. Despite the existence of delocalization, C18 is a suitable location for nucleophilic addition due to the presence of benzyl group which could be a better leaving from the molecule. The OH addition structure was optimized; the C1 proton is more stable because it requires less energy (Fig. 9). The -OH addition is further stabilized by creating a hydrogen bond with O16, forming a six-membered cyclic ring. Molecular electrostatic potential (MEP) analysis provided additional evidence to support the OH addition phenomenon (Fig. 9). However, it gives us the opposite result in alkaline pH: fluorescence enhancement was observed instead of quenching. Then, we realized that the intramolecular hydrogen bonding in the form of the five-membered ring will influence fluorescence enhancement. Further, the study was evidenced by the experimental results

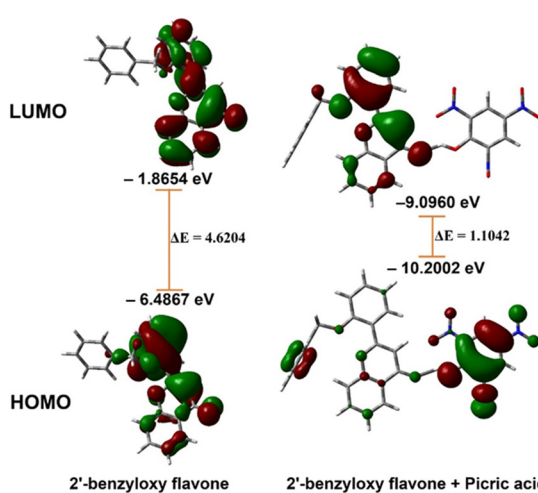


Fig. 7 HOMO and LUMO orbitals of 2-benzyloxy flavone and 2-benzyloxy flavone + picric acid.

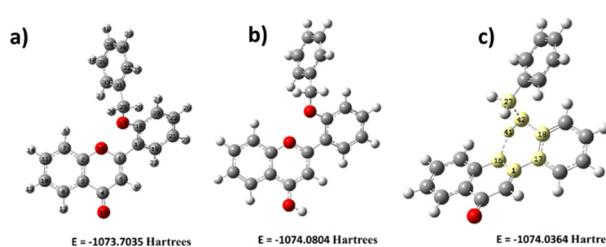


Fig. 8 Energy comparison of proton addition structures (a) without proton addition, (b) with proton addition on carbonyl oxygen, and (c) with proton addition on benzyl oxygen.



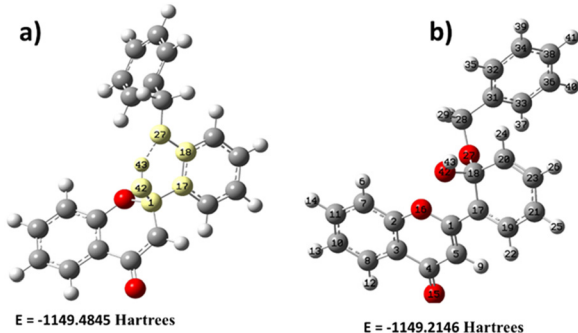


Fig. 9 Energy comparison of hydroxyl (OH) addition of 2'-benzyloxy flavone. (a) OH addition on C1, (b) OH addition on C18.

suggesting that fluorescence enhancement is more pronounced in basic pH than in acidic pH.

### 3.8. Molecular electrostatic potential analysis (MEP)

MEP is a valuable tool for examining chemical reactivity sites, such as electrophilic and nucleophilic regions in molecular systems. The MEP tool can identify binding sites, charge distribution, and electrostatic potential. The MEP surface (Fig. 10) has a variety of colors, from red to blue. Red indicates nucleophilic reactivity, while the blue parts show electrophilic reactivity.<sup>42,43</sup> These observations suggest that the carbonyl oxygen (O4) has a higher electron density than the other two oxygen atoms (O16 and O27 in Fig. 10). These three oxygens are potential electropositive binding sites. Moreover, the electropositive areas are mainly around the hydrogen atoms and phenyl rings.

### 3.9. TD-DFT calculation

2'-Benzylxy flavone exhibits a striking  $\pi-\pi^*$  and  $n-\pi^*$  type transition from the lowest unoccupied molecular orbital (LUMO 87) to the highest occupied molecular orbital (HOMO 82) at 316 nm with an oscillation strength of 0.0389. The theoretical adsorption and emission spectra data and vertical excitation are shown in Table 1 and Fig. 11.

The local HOMO electron is a delocalized benzyl ring with a minor delocalization on the flavone ring. This benzyl-delocalized electron (HOMO) completely passes to the flavone ring during the local transition. The second transition, from

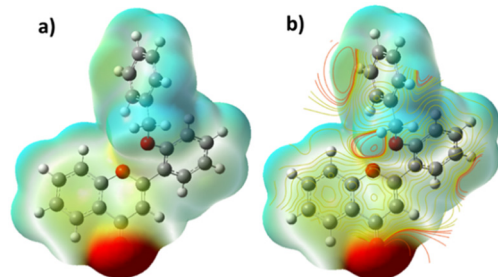


Fig. 10 MEP surface of the 2'-benzyloxy flavone. (a) MEP surface, (b) MEP surface with contour.

Table 1 Excitation energy, oscillator strength, and electronic configuration of 2'-benzyloxy flavone

$E$ (eV)	$\lambda$ (nm) cal	$f$	Configurations	$\lambda$ (nm) expt.
Absorption ( $S_0 - S_1$ )				
3.79	326.74	0.1281	HOMO $\rightarrow$ LUMO (73.36%)	
3.91	316.79	0.0389	HOMO-4 $\rightarrow$ LUMO (33.10%)	310
4.26	290.41	0.1146	HOMO-1 $\rightarrow$ LUMO (90.13%)	290
Emission ( $S_1 - S_0$ )				
2.36	524.16	0.0000	HOMO $\rightarrow$ LUMO (71.16%)	427
3.43	360.52	0.0000	HOMO-3 $\rightarrow$ LUMO + 10 (5.70%)	
3.45	359.08	0.0000	HOMO-5 $\rightarrow$ LUMO (7.66%)	

HOMO (85) to LUMO (87), occurs at 290 nm and has an energy gap of 4.26 eV. In the ground state, the HOMO (85) electron is delocalized in the A and C rings of the flavone moiety, when the transition occurs, the electron is distributed throughout the molecule. The third lower energy transition involving phenyl ring B and the  $\alpha, \beta$  unsaturated double bond (HOMO 86) to phenyl ring A (LUMO 87) occurs at 326 nm. The 2-benzylxy flavone displayed emission at 524 nm (2.36 eV) associated with the LUMO to HOMO transition with an oscillator strength of zero and 71% orbital contribution in the emission TD-DFT spectra calculation, which is somewhat closer to the experimental emission spectra.

### 3.10. Selectivity study of picric acid and other nitroaromatics

After evidencing the chemistry between fluorophore and picric acid (from both theory and experiment), it is important to know whether other nitroaromatics also affect the present fluorophore system. From the DFT study, it is identified that both flavone and picric acid have proton donor-accepting properties. The question remains whether the compound does not possess acidic proton (hydroxyl group) differentiation (Fig. 12A and B). Different nitroaromatic compounds were taken for the quenching studies. Surprisingly, we found that other

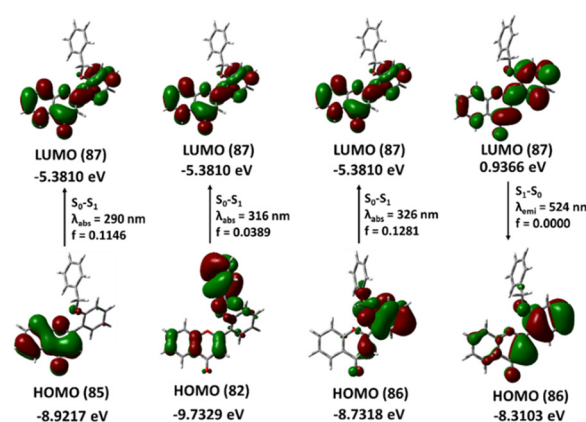
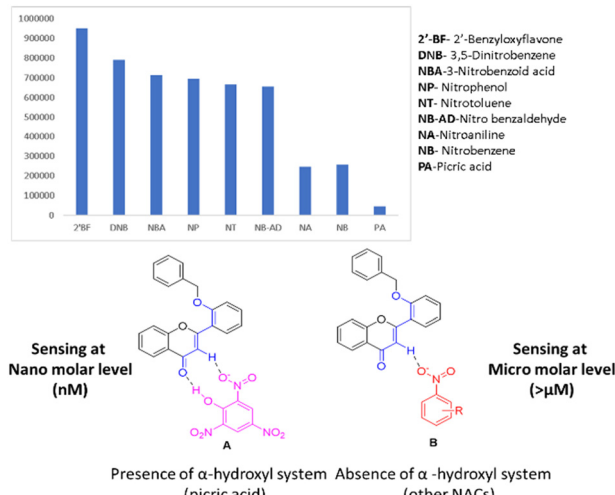


Fig. 11 The frontier molecular orbitals involved in the vertical excitation of 2'-benzyloxy flavone.





**Fig. 12** Selectivity study of picric acid and other nitroaromatics on fluorophore, A) interaction of fluorophore with picric acid and B) interaction of fluorophore with other NAs.

nitroaromatics lacking alpha-acidic protons had fewer quenches when compared to picric acid. The fluorophore quenching is due to the acidic nature of the  $\alpha$ -hydrogen in the flavone moiety. However, these compounds do not show a quenching effect as compared to picric acid (which has an acidic proton). This effect could be due to the proton-accepting nature of carbonyl oxygen from flavone moiety, which proves the effect of picric acid on the fluorophore system. The results indicated that picric acid is selective, and only 300 nM is needed to achieve this complete quenching effect. Hence, picric acid is more effective in quenching flavone fluorophore than other nitroaromatics (Fig. 12).

NAs were tested for the minimum quantity required for effective fluorophore quenching and it was found that all other nitroaromatics needed a 40 micromolar minimum quantity for effective fluorophore quenching. Benzaldehyde was taken as a negative control to prove the no-quenching effect of the fluorophore. Also, the prepared fluorophore can detect various pH under normal conditions. Screening different nitroaromatics for fluorophore quenching leads to the identification of novel fluorophores for selective sensors for picric acid.

The fluorescence enhancement at pH 3 and fluorescence quenching in the presence of picric acid were further evaluated by quantum yield measurement. In this measurement, quinine sulfate was used as a reference. The probe showed a quantum yield of  $\phi_f = 0.9838$  in the presence of acid, and the presence of picric acid quantum yield of  $\phi_f = 0.994$  and  $\phi_f = 0.2195$ , respectively. A significant change was found in the presence of acid due to local environmental changes in fluorophore, which means that fluorophore electron density interacts with the proton. The quantum yield  $\phi_f = 0.7643$  decreased in the presence of picric acid, which is due to the diminishing nature of the fluorophore in the presence of picric acid. Quantum yield measurement further

evidenced the stronger binding nature of the probe toward picric acid.

## 4. Conclusion

The design and synthesis of 2'-benzyloxy flavone has been developed as a dual fluorophore for the detection of secondary explosives, such as picric acid, and pH sensing. Amongst the nitroaromatics tested, it is found to be selective for picric acid at the nanomolar level. The study on real water samples showed that minimum interferences have been identified which can be extended for environmental applications. Further, the synthesized fluorophore is effective in monitoring wide ranges of pH from 1 to 14. In addition, the analysis was carried out in fluorophore-based paper to develop a smart testing module for the dual sensing analysis. The DFT study further supports the quenching activity of picric acid on the selective sensing of picric acid, among others. Since 2'-benzyloxy flavone is non-toxic to cells, it can be taken for biomarkers with activities in the biological system; studies are now in progress. The present system can be tuned for different sensing applications from material to biomedical due to the multiple sites of the flavone scaffold. Also, it is extended to improve trace detection of various nitro-substituted derivatives.

## Data availability

Data files can be shared on reasonable request.

## Author contributions

PN and SS contributed to the conceptualization, design, and writing of the manuscript. VG executed the experiments, DFT calculation, and writing of the manuscript. JS and NR equally contributed to this article by carrying out the quenching experiment of picric acid with the analyte. TKM, ARK, and AON carried out the synthesis and purification of the fluorophore. PM and TM analyzed the data.

## Conflicts of interest

There are no conflicts to declare.

## Acknowledgements

Dedicated to the memory of Prof. Asoke Banerji, who is a guiding light.

## Notes and references

1. M. Shellaiah, Y. T. Chen, N. Thirumalaivasan, B. Aazaad, K. Awasthi, K. W. Sun, S. P. Wu, M. C. Lin and N. Ohta, *ACS Appl. Mater. Interfaces*, 2021, **13**, 24.
2. J. Pan, F. Tang, A. Ding, L. Kong, L. Yang, X. Tao, Y. Tiana and J. Yang, *RSC Adv.*, 2015, **5**, 191.
3. B. W. Xu, X. F. Wu and H. B. Li, *Macromolecules*, 2011, **44**, 5089.



4 F. Zhang, L. Luo and Y. Sun, *Tetrahedron*, 2013, **69**, 9886.

5 P. Jana, M. Yadav, T. Kumar and S. Kanvah, *J. Photochem. Photobiol. A*, 2021, **404**, 112874.

6 A. Karpe, A. Parab, G. Ganesan, P. Walke and A. Chaskar, *J. Photochem. Photobiol. A*, 2022, **431**, 114004.

7 M. Shellaiah, T. Simon, V. Srinivasadesikan, C. M. Lin, K. W. Sun, F. H. Ko, M. C. Lin and H. C. Lin, *J. Mater. Chem. C*, 2016, **4**, 2056.

8 Q. M. Andersen and K. R. Markham, *Flavonoids; Chemistry, Biochemistry, and Applications*, CRC Press, Taylor & Francis Group, 6000 Broken Sound Parkway NW, Suite 300, Boca Raton, FL 33487-2742, 2006.

9 T. J. Mabry, K. R. Markham and M. B. Thomas, *The systematic identification of flavonoids*, Springer-Verlag, Berlin, Heidelberg, New York, 1970.

10 E. Corradinia, P. Fogliaa, P. Giansantia, R. Gubbiottia, R. Samperia and A. Laganà, *Nat. Prod. Res.*, 2011, **25**, 469.

11 K. Ponnvel, G. Banupriya and V. Padmini, *Sens. Actuators, B*, 2016, **234**, 34.

12 Z. Luo, B. Liu, S. Si, Y. Lin, C. S. Luo, C. Pan, C. Zhao and L. Wang, *Dyes Pigm.*, 2017, **143**, 463–469.

13 N. Pandurangan, C. Bose and A. Banerji, *Bioorg. Med. Chem. Lett.*, 2011, **21**, 5328.

14 S. Kumar and A. K. Pandey, *Sci. World J.*, 2013, DOI: **10.1155/2013/162750**.

15 Y. Wang, K. K. J. Chan and W. Chan, *J. Agric. Food Chem.*, 2017, **65**, 4255.

16 J. Lewkowski, D. Rogacz and P. Rychter, *Chemosphere*, 2019, **222**, 381e390.

17 S. Y. Oh, J. G. Son and P. C. Chiuz, *Environ. Toxicol. Chem.*, 2023, **32**, 501.

18 S. Shanmugaraju and P. S. Mukherjee, *Chem. Commun.*, 2015, **51**, 16014.

19 S. O. Tümay and S. Yeşilot, *Sens. Actuators, B*, 2021, **343**, 130088.

20 A. U. Alama, Y. Qina, S. Nambiarc, T. W. John, Y. M. M. R. Howladera, H. Nan-Xing and M. J. Deen, *Prog. Mater. Sci.*, 2018, **96**, 174–216.

21 M. Shamsipure, A. Barati, Z. Nematifar and K. Iran, *J. Photochem. Photobiol. C: Photochem. Rev.*, 2019, **39**, 76.

22 M. Martineau, A. Somasundaram, J. B. Grimm, T. D. Gruber, D. Choquet, J. W. Taraska, L. D. Lavis and D. Perrais, *Nat. Commun.*, 2017, **8**, 1412.

23 Y. Zhan, L. Lin, M. Chen and L. Wu, *ACS Appl. Mater. Interfaces*, 2018, **10**, 33390.

24 C. McDonagh, C. S. Burke and B. D. MacCraith, *Chem. Rev.*, 2008, **108**, 400.

25 D. Wencel, T. Abel and C. McDonagh, *Anal. Chem.*, 2014, **86**, 15.

26 B. Schyrr, S. Pasche, E. Scolan, R. Ischer, D. Ferrario, J. A. Porchet and G. Voirin, *Sens. Actuators, B*, 2014, **194**, 238.

27 Z. Yang, W. Qin, J. W. Y. Lam, S. Chen, H. H. Y. Sung, I. D. William and B. Z. Tang, *Chem. Sci.*, 2013, **4**, 3725.

28 J. Qi, D. Y. Liu, X. Liu, S. Guan, F. Shi, H. Chang, H. He and G. Yang, *Anal. Chem.*, 2015, **87**, 5897.

29 D. Merli, S. L. Cognata, F. Balduzzi, A. Miljkovic, L. Toma and V. Amendola, *New J. Chem.*, 2018, **42**, 15460.

30 E. A. Kataev, *Chem. Commun.*, 2023, **59**, 1717.

31 S. L. Cognata and V. Amendola, *Chem. Commun.*, 2023, **59**, 13668.

32 N. Pandurangan, N. Jyotsna, G. B. Nair and A. Banerji, *Bioorg. Med. Chem.*, 2015, **23**, 3781.

33 V. S. Patil, V. S. Padalkar, A. B. Tathe, V. D. Gupta and N. Sekar, *J. Fluoresc.*, 2013, **23**, 1019.

34 S. Gharbi, K. Hriz and M. Majdoub, *Opt. Mater.*, 2023, **137**, 113537.

35 S. Biswas, A. Pramanik, S. Pal and P. Sarkar, *J. Phys. Chem. C*, 2017, **121**, 2574.

36 G. Venkatesh and M. Sundaravadivelu, *Res. Chem. Intermed.*, 2019, **45**, 4395.

37 K. Anandhan, M. Ceron, V. Perumal, P. Ceballos, P. Gordillo-Guerra, E. Perez-Gutierrez, A. E. Castillo, S. Thamotharan and M. J. Percino, *RSC Adv.*, 2019, **9**, 12085.

38 A. S. Tanwar, R. Parui, R. Garai, M. A. Chanu and P. K. Iyer, *ACS Meas. Sci. Au*, 2022, **2**, 23–30.

39 M. Shellaiah, K. Awasthi, S. Chandran, B. Aazaad, K. W. Sun, N. Ohta, S. P. Wu and M. C. Lin, *ACS Appl. Nano Mater.*, 2022, **5**, 2859–2874.

40 C. Nandhini, P. S. Kumar, R. Shanmugapriya, K. N. Vennila, G. Abdullah, A. Sehem, M. Pannipara and K. P. Elango, *J. Mol. Struct.*, 2022, **1268**, 133685.

41 S. El Behi, S. Ayachi and S. Znaidia, *J. Mol. Liq.*, 2022, **360**, 119550.

42 C. H. Suresh, G. S. Remya and P. K. Anjalikrishna, *Comput. Mol. Biosci.*, 2022, e1601.

43 G. Venkatesh and M. Sundaravadivelu, *J. Mol. Struct.*, 2021, **1229**, 129653.

